Understanding Gas-Induced Structural Deformation of ZIF-8

ARTICLE *in* JOURNAL OF PHYSICAL CHEMISTRY LETTERS · MAY 2012

Impact Factor: 7.46 · DOI: 10.1021/jz300292y

THE JOURNAL OF PHYSICAL CHEMISTRY Letters

Letter

pubs.acs.org/JPCL

Understanding Gas-Induced Structural Deformation of ZIF-8

Conchi O. Ania,*[,‡] E. García-Pérez,[†] M. Haro,[‡] J. J. Gutiérrez-Sevillano,[†] T. Valdés-Solís,[‡] J. B. Parra,[‡] and S. Calero*[,†]

[†]Departamento Sistemas Físicos, Químicos y Naturales. Universidad Pablo de Olavide, Carretera de Utrera, km. 1, 41013 Sevilla, Spain

[‡]Departamento de Procesos Químicos en Energía y Medio Ambiente, Instituto Nacional del Carbón (INCAR-CSIC), P.O. 73, 33080 Oviedo, Spain

Supporting Information

ABSTRACT: ZIF-8 is a zeolitic imidazolate framework with very good thermal and chemical stability that opens up many applications that are not feasible by other metal−organic frameowrks (MOFs) and zeolites. Several works report the adsorption properties of ZIF-8 for strategic gases. However, despite the vast experimental corpus of data reported, there seems yet to be a dearth in the understanding of the gas adsorption properties. In this work we provide insights at a molecular level on the mechanisms governing the ZIF-8 structural deformation during molecular adsorption. We demonstrate that the ZIF-8 structural deformation during the adsorption of different molecules at cryogenic temperature goes beyond the gas-induced rotation of the imidazolate linkers. We combine experimental and simulation studies to demonstrate that this deformation is governed by the polarizability and molecular size and shape of the gases, and that the stepped adsorption behavior is defined by the packing arrangement of the guest inside the host.

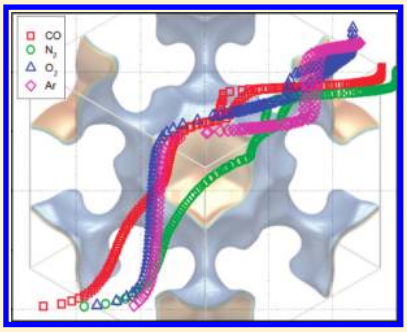

SECTION: Surfaces, Interfaces, Porous Materials, and Catalysis

Zeolitic imidazole frameworks (ZIFs) represent a new family of porous crystalline materials, recently synthesized by Yaghi and co-workers,[1,2] consisting of tetrahedral units where bivalent transition metals are coordinated to imidazolate ligands. Along with well-defined pore architectures, these materials combine large chemical and thermal stability anticipating promising applications in catalysis and gas storage and separation.[3−5]

Among them, Zn(2-methylimidazole)$_2$ (ZIF-8) is a prototypical compound that has a sodalite zeolite-type structure where the imidazolate linkers form large cages connected through narrow windows.[2,6] The outstanding thermal and chemical stability of ZIF-8 opens up many applications that are not feasible by many other metal−organic frameworks (MOFs) and zeolites. Driven by these chemical and structural features, a substantial number of works report the adsorption properties of ZIF-8 for a variety of strategic gases (CO_2, CH_4, H_2)[7,8]as well as other polar and nonpolar probes (methanol, propylene, ethylene).[1] Despite the vast experimental corpus of data that has been reported, there seems yet to be a dearth in the understanding of the gas adsorption properties. For instance, the experimental adsorption and diffusion of molecules in which the kinetic diameter is larger than the dimensions of the pore aperture has suggested some flexibility in the structure of several ZIFs,[6,9,10] albeit considered rigid.[2] This behavior has been recently attributed to the freedom of the imidazolate linkers to rotate over a certain angle, allowing large molecules to enter the main cavities.[6,9,10] The interactions between the linker and the adsorbate seem to control the threshold pressure of the gate-opening behavior and, consequently, the uptake and release of the adsorbed gas molecules.[11]

In this work we provide insights at a molecular level on the mechanisms governing the ZIF-8 structural deformation during the adsorption of different molecules, showing that this phenomenon goes beyond the gas-induced rotation of the imidazolate linkers. We have explored the gas adsorption behavior of ZIF-8 by measuring high-resolution adsorption isotherms of N_2, O_2, Ar, and CO at cryogenic temperatures. The choice of the gases was made based on their distinctive size, shape, and polarity.

The adsorption isotherms at 77 K of the studied gases on ZIF-8 are shown in Figure 1. Three different regions, characterized by multistep adsorption features and hysteresis in the desorption branch, can be clearly distinguished for the studied gases. According to the literature, this behavior is characteristic of flexible host materials where adsorption proceeds by a sequential filling of the main cavities. Indeed, the stepped adsorption behavior of ZIF-8 has already been reported for N_2 and Ar.[2] What seems interesting to remark is the distinct adsorptive behavior of the studied gases, which has not yet been fully understood. Several scenarios could be speculated for its interpretation, including gas-induced

Received: March 12, 2012
Accepted: April 12, 2012
Published: April 12, 2012

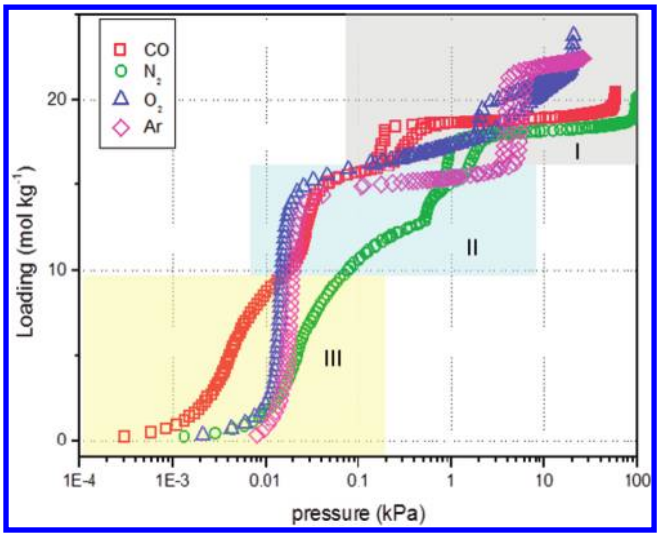

Figure 1. Experimental equilibrium adsorption isotherms at 77 K of N_2, CO, Ar, and O_2 on ZIF-8. Regions I, II, and III are colored in gray, light blue, and light orange, respectively.

flexibility of the framework, reorganization of the adsorbed molecules, polarizability effects, different adsorption sites depending on the nature of the gas, or size and shape effects of the gas molecules.[2,12] To clarify the most likely scenario governing ZIF-8 adsorption features, we have analyzed the adsorption isotherms combining experimental and molecular simulation approaches.

ZIF-8 was modeled as a rigid structure. The crystalline structures corresponding to ZIF-8 were optimized in vacuum (VS) and at high pressures (HP) after deformation at 1.47 GPa in the presence of a hydrostatic medium.[12]

Data corresponding to the adsorption saturation capacities of all the studied gases using both structures (Table 1) show that predicted capacities using VS structure underestimate the experimental values, whereas computed values using the HP structure are overestimated. This indicates that even though gas-induced structural deformation of ZIF-8 framework upon gas loading is confirmed (at 77 K and atmospheric pressure), it occurs to a lower extent than that reported after applying 1.47 GPa to the structure.

The structural deformation of ZIF-8 was also confirmed by the computed equipotential energy surfaces (Figure 2) of both VS and HP structures; an expansion of the main cavities of ZIF-8 was obtained when the gas loading was above a threshold value, also accompanied by an enlargement and twist of the connecting windows, which leaves a higher volume accessible to gases and thus accounts for the increase in amount adsorbed in the HP structure (Table 1).

The average occupation profiles obtained from VS and HP structures (Figures S1 and S2 in the Supporting Information) also confirmed the lack of preferential adsorption sites for any of the studied gases. These profiles show atoms located at the pore openings connecting the cavities regardless the nature of the gas; this seems reasonable considering the high symmetry of the structure of ZIF-8 and the fact that adsorption is favored due to confinement effects. Bearing this in mind, the scenario based on different adsorption sites accounting for the multistepped adsorption behavior of these gases can be discarded, and differences should be attributed to the shape and/or polarity of the gases (through gas-gas or gas-host interactions), as it will be discussed below.

Region I in Figure 1 shows an adsorption substep for all the gases, although at different threshold pressures for all of them. We attribute this behavior to the expansion of the porous framework after the structural deformation. In the case of Ar and O_2, the substep accounts for a 1.5-fold increase in the amount of gas adsorbed. This suggests that when the gas loading is high, the adsorbed molecules already filling the cavities could be able to open-up the structure for accommodating a higher number of molecules. As mentioned above, according to the average occupational profiles, the atoms are located mostly at the entrance of the main cavities (Figure S2); thus due to confinement effects, the adsorbed molecules lock/block the connecting windows preventing the expansion (deformation) of the structure until a given pressure (loading) is reached. The onset pressure for the opening effect in the adsorption branch is about the same for Ar than for O_2, although it accounts for higher oxygen loading, which is reasonable considering its smaller dimension. Additionally, the gas uptake after the opening of the structure is rather steep for Ar, suggesting a close packing arrangement of the argon molecules inside the gas induced void. In the case of O_2, the second adsorption substep is smoother, which indicates the occurrence of O_2-framework interactions likely as a consequence of its quadrupolar moment. Figure 3 shows that the structural opening is not only related to the nature of the gas, but is also highly temperature dependent. Indeed, the isotherms at 77 and 90 K are essentially identical, and the adsorption substeps occur at approximately the same gas loadings but shifted toward higher pressures. This trend was observed for all the gases, thus confirming the temperature dependence of the opening/closing process.

For CO and N_2, an adsorption substep was observed in region I at onset pressures of ca. 0.2 and 1 kPa, respectively (before the plateau corresponding to the saturation point). Considering the polarity of CO and N_2, it is plausible to speculate that some electrostatic effects might arise between the dipolar/quadrupolar moments of the gases and the ZIF-8 framework. These would determine the packing arrangement of the adsorbed gas molecules. Thus, the opening effect induced by polar gases would show a two-step transition (rather than the single step observed for Ar and O_2). When the gas loading is high enough to promote the expansion of the structure, gas−gas and gas−host interactions become important; based on these specific interactions for polar probes, a certain packing reorganization of the adsorbed molecules would occur,

Table 1. Experimental and Simulated Saturation Capacities in Molecules Per Unit Cell at 77 K

	N_2	O_2	Ar	CO
simul (VS)[a]	45.93 ± 0.16	59.96 ± 0.10	56.42 ± 0.23	45.91 ± 0.31
simul (HP)[b]	56.52 ± 0.15	65.90 ± 0.21	65.99 ± 0.01	54.10 ± 0.11
experiment	55.00 ± 0.02	64.83 ± 0.04	61.37 ± 0.02	55.32 ± 0.01

[a]VS = optimized vacuum structure.[12] [b]HP = high pressure structure optimized after deformation at 1.47 GPa.[12,13]

dx.doi.org/10.1021/jz300292y | J. Phys. Chem. Lett. 2012, 3, 1159−1164

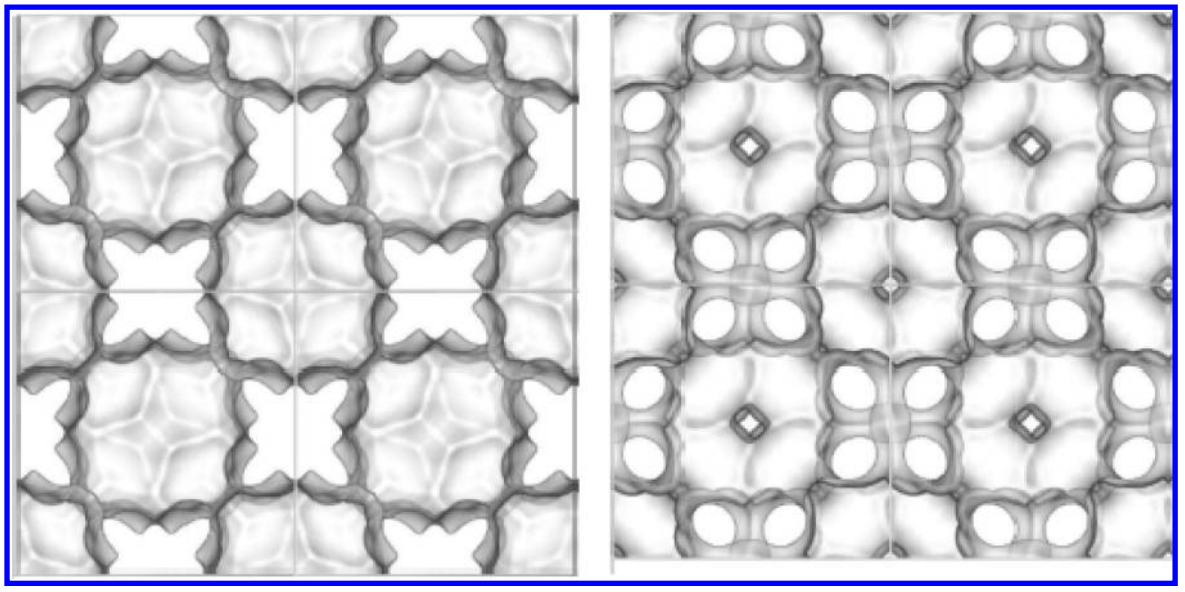

Figure 2. Equipotential energy surfaces along the *x* axis in the VS (left) and HP (right) ZIF-8 structures.

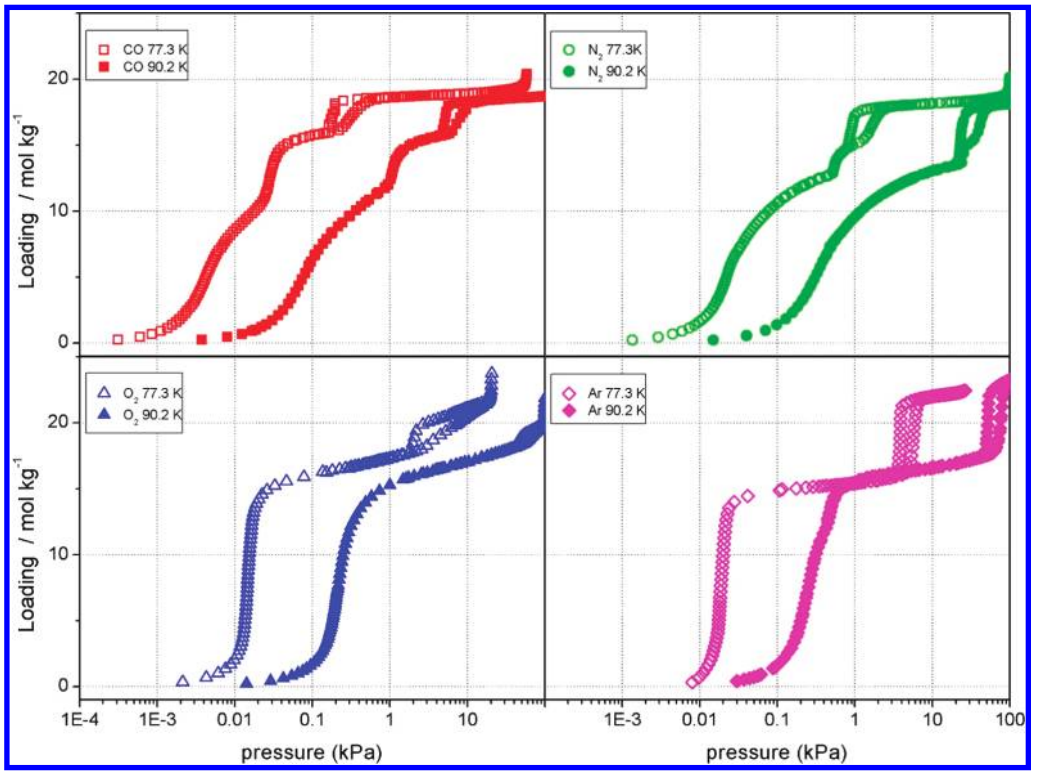

Figure 3. Experimental equilibrium adsorption isotherms at 77 and 90 K, illustrating the temperature dependence of the structural opening. Top left: CO; top right: N_2; bottom left: O_2; bottom right: Ar.

accounting for the sloping and stepped features of CO and N_2 adsorption isotherms in regions I and II. Unlocking of ZIF-8 openings would be delayed by the low adsorption potential of the transition phase provoked by the polar interactions; at a certain point, the loading becomes so high that deformation of the structure is forced. Experimentally, a remarkable increase in the recorded adsorption equilibrium time was observed in this region (delayed/slow opening), which would confirm the hypothesis. This behavior could be considered as analogous to the breathing process featuring structural transitions between the np and lp forms reported for MIL-53.[14]

High-resolution adsorption isotherms at cryogenic temperature also revealed interesting desorption features in region I, with hysteresis loops in the desorption branch for all the studied gases. Although a hysteretic behavior has been reported for Ar adsorption at 87 K,[2] this finding contrasts with the number of experimental data reporting reversible adsorption/desorption behavior of N_2 at 77 K in ZIF-8.[12,15] What is important to highlight is that, for all the studied gases, the hysteresis corresponds to desorption of the molecules accommodated in the framework after opening of the structure. As also pointed out in the adsorption branch, hysteresis

dx.doi.org/10.1021/jz300292y | J. Phys. Chem. Lett. 2012, 3, 1159−1164

desorption was accompanied by a remarkable increase in the equilibrium time.

The onset and closing pressure points of the hysteresis loops are too low to be associated with capillary condensation in mesopores; thus it is plausible to attribute this behavior to the structural transition of the framework and the reorganization of the remaining adsorbed molecules, while desorbing from the expanded ZIF-8 structure. Indeed, similar low pressure hysteresis behaviors have been reported for zeolites and MOFs.[9,12,16] It is worth mentioning that for all of them, only one desorption loop was detected, at least up ca. 0.01 kPa, the lowest pressure limit recorded in our desorption experiments.

In the case of N_2 and CO, two more substeps can be observed at gas loadings above 10 mol/kg (region II in Figure 1), which we attribute to the gas-induced opening of the ZIF-8 structure. This substep in region II is much more evident for CO (loading ca. 30 molec/uc), and appears at an onset pressure of 1 order of magnitude lower than of N_2 (loading ca. 35 molecule/uc). The experimental values concerning opening pressure and loadings herein determined for N_2 are in good agreement with those reported in the literature.[12]

It should also be noted that the sequence of the opening pressure corresponding to this adsorption substep (region II) correlates well with the gas adsorption strength (increasing adsorption strength decreases the opening pressure in the order CO < N_2 < O_2 ~ Ar) and the size of the probes (for smaller gases, higher loadings are needed to open the structure). It is also interesting to point out that in the case of CO and N_2, deformation of the ZIF-8 structure allows nearly doubling the amount of adsorbed gas (Figure 1).

Finally, significant differences are also observed in region III, corresponding to Henry's law regime (low gas loadings). A sharp vertical adsorption substep is observed for Ar and O_2 from 0.01 kPa, whereas for the same region the uptake starts from lower onset values of pressure for CO and N_2, and it proceeds much more gradually and weakly with pressure. A similar substep reaching a plateau has been reported by Yaghi et al. for Ar at 87 K.[2] The logic of such adsorption behavior in low pressure regime (region III) seems to be related to the size and geometry of the gases rather than to their chemical properties (polarity). Indeed, the steep adsorption substeps observed for Ar and O_2 suggest that both molecules do not have any restriction to access ZIF-8 cavities, and that there is no preferential adsorption sites for these probes. In other words, primary filling of ZIF-8 cavities proceeds by a close-packing arrangement of both gas molecules. This theory is also corroborated with the simulation of adsorption isotherms with a controlled decrease of the sigma Lennard-Jones parameter for argon, moving from 3.38 Å to 2 Å. Simulations (Figure S3, Supporting Information) show the steep adsorption for all sigma values considered. This seems reasonable since specific (electrostatic) adsorbate−framework or adsorbate−adsorbate interactions would not be expected for non-polarizable gases. Moreover, a well-defined plateau (region II) is reached for Ar and O_2 at loadings of ca. 15−18 mol/kg (pressures between 0.1 and 1 kPa), after which the uptake increases much more weakly with pressure.

In the case of N_2 and CO, the uptake in region III follows a rather similar trend, although the adsorption process is much more gradual and sloping. In both cases, the adsorption starts at lower onset pressures due to the adsorption enhancement of polar molecules (CO and N_2 show dipolar and quadrupolar moments). The sloping shape of these isotherms suggests a different reorganization inside the cavities of ZIF-8, compared to Ar and O_2; however the average occupation profiles corresponding to region III obtained from molecular simulations (Figure S1) confirmed the lack of preferential adsorption sites for any of the studied gases, with atoms located at the pore openings (windows) connecting the cavities regardless the nature of the gas. Thus, differences observed in the adsorption behavior should be attributed to the shape and/or polarity of the gases (through gas−gas or gas−host interactions).

This first substep at low gas loadings (region III) was predicted by molecular simulation using the force field corresponding to the VS structure (Figure S4). Despite the lack of good force fields able to accurately reproduce the isotherms, there is a reasonable agreement between experimental and simulation data. This confirmed that no structural deformation of ZIF-8 has yet occurred in region III for any of the studied gases.

To further investigate the different adsorptive behavior of the studied gases in region III, adsorption was computed modifying the fitting Lennard-Jones and charge parameters of the gases (Figure 4). Computed data revealed no adsorption changes in region III when the gases were deprived of their quadrupolar/dipolar moments; in contrast, modification of Lennard-Jones parameters drastically changed the adsorption behavior. When O_2 was modeled using the Lennard-Jones parameters of N_2 (i.e., making O_2 bigger), the adsorption changed from the steep vertical isotherm (experimentally observed for O_2) to the sloping one (experimentally observed for CO and N_2). This confirms that adsorption on the low gas loading region is governed by the packing arrangement of the probes rather than their polarizability: oxygen and argon fit better in the cavities due to their adequate (small) dimensions and geometry, whereas large nitrogen and carbon monoxide pack worse in the structure.

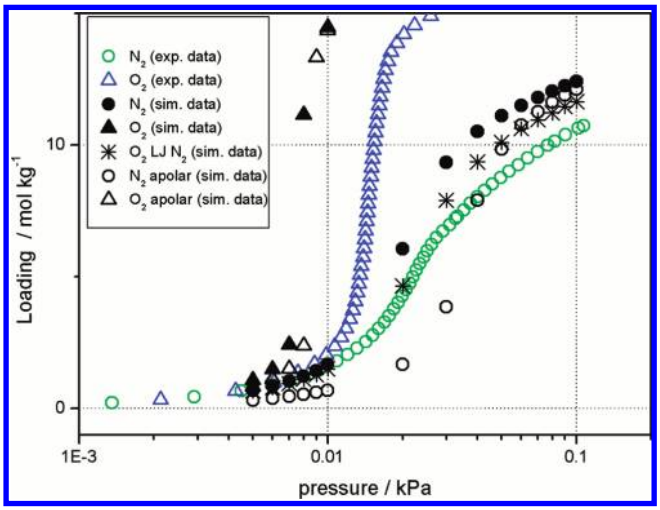

Figure 4. Simulated adsorption isotherms at 77 K of N_2 and O_2 on ZIF-8.

We have demonstrated that the ZIF-8 structural deformation during the adsorption of different molecules at cryogenic temperatures goes beyond the gas-induced rotation of the imidazolate linkers. The combination of experimental and simulation studies evidence that this deformation is governed by the polarizability and molecular size and shape of the gases.

dx.doi.org/10.1021/jz300292y | J. Phys. Chem. Lett. 2012, 3, 1159−1164

This study also demonstrates that the stepped adsorption behavior is defined by the packing arrangement of the guest inside the host, which in turn determines how the adsorbed gas molecules distribute inside the cavities and control the gas-induced opening of the ZIF-8 structure. Gas−framework electrostatic interactions become important for polar molecules, defining the multistepped features observed, for instance, in CO and N_2, and enabling delayed opening of the structure.

High-resolution adsorption isotherms have revealed a hysteretic desorption behavior in ZIF-8, indicating that knowledge on basic adsorption properties of this singular material has very often been based on incomplete experimental data.

EXPERIMENTAL AND SIMULATION SECTION

High-resolution gas adsorption isotherms at 77 and 90 K (liquid nitrogen and liquid oxygen baths, respectively) were carried out in a Micromeritics ASAP2020 HD Instrument in the pressure range from 10^{-4} to 120 kPa. The instrument was equipped with a molecular drag vacuum pump and three different pressure transducers (0.0133, 1.33 and 133 kPa, uncertainty within 0.15% of reading) to enhance the sensitivity in the low-pressure range, which is especially useful in adsorption studies on highly microporous materials. Powders of ZIF-8 were transferred to a preweighed analysis tube, which was capped with a sealed frit and outgassed under dynamic vacuum (ca. 10^{-5} Torr) at 120 °C overnight. The evacuated analysis tube containing the evacuated sample was transferred to an electronic balance and weighed again to determine the mass of sample (ca. 200 mg); the tube was then transferred back to the analysis port of the gas adsorption instrument. Strict analysis conditions were programmed during the gas adsorption measurements to ensure equilibrium data in all gases. Consequently, the average elapsed time for the measurement of the isotherms was 90−120 h, with over 100 equilibrium points. The saturation pressures of the corresponding gases were continuously measured throughout the analysis by means of a pressure transducer; the nonideality factors were 6.3×10^{-5} (Ar), 6.5×10^{-5} (O_2), 5.9×10^{-5} (N_2), and 7.1×10^{-5} (CO). All the gases were supplied by Air Products with an ultrahigh purity (i.e., 99.9992%). For all isotherms, warm and cold free-space correction measurements were performed by using ultrahigh purity He gas (grade 5.0, 99.999% purity).

The computed adsorption isotherms were obtained using Monte Carlo in the Grand-Canonical ensemble. The Monte Carlo moves were performed in cycles, and in each cycle one move was chosen at random with a fixed probability of translation, rotation, and regrowth in a random position. At least 10^7 cycles were used, and charge interactions were computed using Ewald sums with a relative precision of 10^{-6}. The Lennard-Jones potentials were cut and shifted with the cutoff distance set to 12 Å. The ZIF-8 structures were modeled as rigid from the crystalline structures taken from the ref 12. The simulation cells were formed by eight unit cells of the VS structure ($a = b = c = 16.993$ Å) and eight unit cells of the HP structure ($a = b = c = 17.071$ Å). The charges and intermolecular parameters for the molecules were developed and validated in previous works,[16−20] and those for the structure were taken from the DREIDING and UFF force fields.[21,22] Lorentz−Berthelot mixing rules were used to calculate mixed Lennard-Jones parameters. All charges and intermolecular parameters used in this work are listed in Table S1 in the Supporting Information.

ASSOCIATED CONTENT

Supporting Information

Table S1 shows the partial charges and Lennard-Jones parameters for the adsorbed molecules used in this work. In Figure S1 the average occupation profiles corresponding to the VS structure for Ar, CO, N_2, and O_2, obtained from molecular simulations are shown; Figure S2 shows the average occupational profiles for Ar, CO, N_2, and O_2, obtained from molecular simulations in the HP structure. Figure S3 shows the effect of the variation of the sigma Lennard-Jones parameter, in Å, on the computed adsorption isotherms of Ar at 77 K. In Figure S4 the computed adsorption isotherms of N_2, CO, Ar and O_2 on ZIF-8 at 77 K are shown. This information is available free of charge via the Internet at http://pubs.acs.org/.

AUTHOR INFORMATION

Corresponding Author

*(C.O.A.) E-mail: conchi.ania@incar.csic.es; Fax: (+34) 985297662. (S.C.) E-mail: scalero@upo.es; Fax: (+34) 954 349 814.

Notes

The authors declare no competing financial interest.

ACKNOWLEDGMENTS

This work is supported by the Spanish MICINN (CTQ2010−16077), by the Junta de Andalucía (P07-FQM-02595), and by the European Research Council (ERC-StG'11 RASPA-project). E.G.-P. and M.H. thank their postdoctoral fellowship to the Spanish Ministerio de Educación and CSIC, respectively, and J.J.G.-S. thanks MEC (CTQ2007-63229) for his predoctoral fellowship.

REFERENCES

(1) Huang, X. C.; Lin, Y. Y.; Zhang, J. P.; Chen, X. M. Ligand-Directed Strategy for Zeolite-Type Metal−Organic Frameworks: Zinc(II) Imidazolates with Unusual Zeolitic Topologies. *Angew. Chem., Int. Ed.* **2006**, *45*, 1557−1559.

(2) Park, K. S.; Ni, Z.; Cote, A. P.; Choi, J. Y.; Huang, R. D.; Uribe-Romo, F. J.; Chae, H. K.; O'Keeffe, M.; Yaghi, O. M. Exceptional Chemical and Thermal Stability of Zeolitic Imidazolate Frameworks. *Proc. Natl. Acad. Sci. U.S.A.* **2006**, *103*, 10186−10191.

(3) Phan, A.; Doonan, C. J.; Uribe-Romo, F. J.; Knobler, C. B.; O'Keeffe, M.; Yaghi, O. M. Synthesis, Structure, and Carbon Dioxide Capture Properties of Zeolitic Imidazolate Frameworks. *Acc. Chem. Res.* **2010**, *43*, 58−67.

(4) Li, J. R.; Kuppler, R. J.; Zhou, H. C. Selective Gas Adsorption and Separation in Metal−Organic Frameworks. *Chem. Soc. Rev.* **2009**, *38*, 1477−1504.

(5) Tran, U. P. N; Le, K. K. A.; Phan, N. T. S. Expanding Applications of Metal−Organic Frameworks: Zeolite Imidazolate Framework ZIF-8 as an Efficient Heterogeneous Catalyst for the Knoevenagel Reaction. *ACS Catal.* **2011**, *1*, 120−127.

(6) Perez-Pellitero, J.; Amrouche, H.; Siperstein, F. R.; Pirngruber, G.; Nieto-Draghi, C.; Chaplais, G.; Simon-Masseron, A.; Bazer-Bachi, D.; Peralta, D.; Bats, N. Adsorption of CO_2, CH_4, and N_2 on Zeolitic Imidazolate Frameworks: Experiments and Simulations. *Chem.—Eur. J.* **2010**, *16*, 1560−1571.

(7) Murray, L. J.; Dinca, M.; Long, J. R. Hydrogen Storage in Metal−Organic Frameworks. *Chem. Soc. Rev.* **2009**, *38*, 1294−1314.

(8) Bux, H.; Chmelik, C.; Krishna, R.; Caro, J. Ethene/Ethane Separation by the MOF Membrane ZIF-8: Molecular Correlation of Permeation, Adsorption, Diffusion. *J. Membr. Sci.* **2011**, *369*, 284−289.

(9) van den Bergh, J.; Gucuyener, C.; Pidko, E. A.; Hensen, E. J. M.; Gascon, J.; Kapteijn, F. Understanding the Anomalous Alkane

Selectivity of ZIF-7 in the Separation of Light Alkane/Alkene Mixtures. *Chem.—Eur. J.* **2011**, *17*, 8832−8840.
(10) Gucuyener, C.; van den Bergh, J.; Gascon, J.; Kapteijn, F. Ethane/Ethene Separation Turned on Its Head: Selective Ethane Adsorption on the Metal−Organic Framework ZIF-7 through a Gate-Opening Mechanism. *J. Am. Chem. Soc.* **2010**, *132*, 17704−17706.
(11) Luebbers, M. T.; Wu, T. J.; Shen, L. J.; Masel, R. I. Effects of Molecular Sieving and Electrostatic Enhancement in the Adsorption of Organic Compounds on the Zeolitic Imidazolate Framework ZIF-8. *Langmuir* **2010**, *26*, 15625−15633.
(12) Fairen-Jimenez, D.; Moggach, S. A.; Wharmby, M. T.; Wright, P. A.; Parsons, S.; Duren, T. Opening the Gate: Framework Flexibility in ZIF-8 Explored by Experiments and Simulations. *J. Am. Chem. Soc.* **2011**, *133*, 8900−8902.
(13) Moggach, S. A.; Bennett, T. D.; Cheetham, A. K. The Effect of Pressure on ZIF-8: Increasing Pore Size with Pressure and the Formation of a High-Pressure Phase at 1.47 GPa. *Angew. Chem., Int. Ed.* **2009**, *48*, 7087−7089.
(14) Ferey, G.; Serre, C. Large Breathing Effects in Three-Dimensional Porous Hybrid Matter: Facts, Analyses, Rules and Consequences. *Chem. Soc. Rev.* **2009**, *38*, 1380−1399.
(15) Chapman, K. W.; Halder, G. J.; Chupas, P. J. Pressure-Induced Amorphization and Porosity Modification in a Metal−Organic Framework. *J. Am. Chem. Soc.* **2009**, *131*, 17546−17547.
(16) Garcia-Perez, E.; Parra, J. B.; Ania, C. O.; Dubbeldam, D.; Vlugt, T. J. H.; Castillo, J. M.; Merkling, P. J.; Calero, S. Unraveling the Argon Adsorption Processes in MFI-Type Zeolite. *J. Phys. Chem. C* **2008**, *112*, 9976−9979.
(17) Martin-Calvo, A.; Garcia-Perez, E.; Garcia-Sanchez, A.; Bueno-Perez, R.; Hamad, S.; Calero, S. Effect of Air Humidity on the Removal of Carbon Tetrachloride from Air Using Cu-BTC Metal−Organic Framework. *Phys. Chem. Chem. Phys.* **2011**, *13*, 11165−11174.
(18) Martin-Calvo, A.; Garcia-Perez, E.; Castillo, J. M.; Calero, S. Molecular Simulations for Adsorption and Separation of Natural Gas in IRMOF-1 and Cu-BTC Metal−Organic Frameworks. *Phys. Chem. Chem. Phys.* **2008**, *10*, 7085−7091.
(19) Garcia-Perez, E.; Gascon, J.; Morales-Florez, V.; Castillo, J. M.; Kapteijn, F.; Calero, S. Identification of Adsorption Sites in Cu-BTC by Experimentation and Molecular Simulation. *Langmuir* **2009**, *25*, 1725−1731.
(20) Calero, S.; Martin-Calvo, A.; Hamad, S.; Garcia-Perez, E. On the Performance of Cu-BTC Metal Organic Framework for Carbon Tetrachloride Gas Removal. *Chem. Commun.* **2011**, *47*, 508−510.
(21) Rappe, A. K.; Casewit, C. J.; Colwell, K. S.; Goddard, W. A.; Skiff, W. M. UFF, a Full Periodic-Table Force-Field for Molecular Mechanics and Molecular-Dynamics Simulations. *J. Am. Chem. Soc.* **1992**, *114*, 10024−10035.
(22) Mayo, S. L.; Olafson, B. D.; Goddard, W. A. Dreiding - A Generic Force-Field for Molecular Simulations. *J. Phys. Chem.* **1990**, *94*, 8897−8909.